Journal of Medicinal Chemistry

ARTICLE

pubs.acs.org/jmc

Symmetric Double-Headed Aminopyridines, a Novel Strategy for Potent and Membrane-Permeable Inhibitors of Neuronal Nitric Oxide Synthase

Fengtian Xue,[†,●] Jianguo Fang,[†,▽] Silvia L. Delker,[§] Huiying Li,[§] Pavel Martásek,[#,¥] Linda J. Roman,[#] Thomas L. Poulos,[*,§,▲] and Richard B. Silverman[*,†,‡]

[†]Department of Chemistry and [‡]Department of Molecular Biosciences, Center for Molecular Innovation and Drug Discovery, Chemistry of Life Processes Institute, Northwestern University, 2145 Sheridan Road, Evanston, Illinois 60208-3113, United States

[§]Department of Molecular Biology and Biochemistry, [▲]Department of Pharmaceutical Sciences, and Department of Chemistry, University of California, Irvine, California 92697-3900, United States

[#]Department of Biochemistry, The University of Texas Health Science Center, San Antonio, Texas 78384-7760, United States

[¥]Department of Pediatrics and Center for Applied Genomics, 1st School of Medicine, Charles University, Prague, Czech Republic

Supporting Information

ABSTRACT: We report novel neuronal nitric oxide synthase (nNOS) inhibitors based on a symmetric double-headed aminopyridine scaffold. The inhibitors were designed from crystal structures of leads **1** and **2** (Delker, S. L.; Ji, H.; Li, H.; Jamal, J.; Fang, J.; Xue, F.; Silverman, R. B.; Poulos, T. L. Unexpected binding modes of nitric oxide synthase inhibitors effective in the prevention of cerebral palsy. J. Am. Chem. Soc. 2010, 132, 5437−5442) and synthesized using a highly efficient route. The best inhibitor, **3j**, showed low nanomolar inhibitory potency and modest isoform selectivity. It also exhibited enhanced membrane permeability. Inhibitor **3j** binds to both the substrate site and the pterin site in nNOS but only to the substrate site in eNOS. These compounds provide a basis for further development of novel, potent, isoform selective, and bioavailable inhibitors for nNOS.

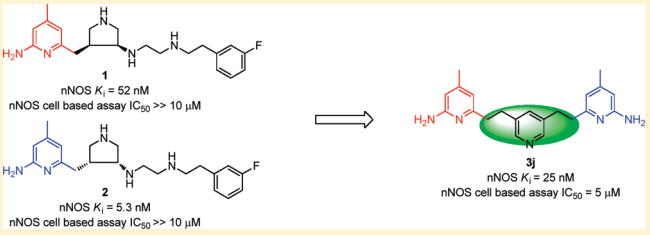

INTRODUCTION

Neurodegenerative disorders, such as Alzheimer's, Parkinson's, and Huntington's disease, have emerged as a rapidly growing age-related health problem in the world. Despite years of efforts invested by scholars in the pharmaceutical and academic community, to date, neurodegeneration caused by various neurodegenerative diseases remains essentially untreatable. Thus, the development of clinically useful therapeutic agents for the affected population has become an urgent need.

Biological studies have demonstrated that overexpression of the neuronal isoform of nitric oxide synthase (nNOS),[1−4] and the subsequent overproduction of the small molecule neurotransmitter nitric oxide (NO), is implicated in various neurological diseases, including Parkinson's,[5] Alzheimer's,[6] and Huntington's diseases,[7] as well as neuronal damage due to stroke.[8] Accordingly, inhibition of the abnormal activity of nNOS has provided a promising target for the development of new therapeutic agents for neurodegeneration.[9−12] In the past two decades, significant research has been devoted to the design and synthesis of potent inhibitors of nNOS.[13−16] Inhibition of nNOS activity has also focused on isoform selectivity over endothelial NOS (eNOS), the NOS isoform that regulates blood pressure and inducible NOS (iNOS), the NOS isoform that plays a critical role in immune responses.[16,17]

Our research group has recently identified a number of chiral pyrrolidine-based inhibitors (**1** and **2**, Figure 1) that possess excellent potency and remarkable isoform selectivity for nNOS over eNOS and iNOS.[17,18] However, results from rodent in vivo studies indicated that these inhibitors have poor ability to penetrate the blood−brain barrier (BBB),[19] which limits their further applications as drug candidates for neurodegenerative diseases. We reasoned that the two high pK_a nitrogen atoms on **1** and **2** (the pyrrolidine nitrogen and the secondary amine in the middle of the alkyl chain) gave them multiple positive charges at physiological pH, which impaired the molecules to diffuse passively into the brain. Moreover, the complex structures of these inhibitors and low overall yield of the syntheses presented additional obstacles to optimizing the pharmacokinetic properties of the inhibitors.[17,19−22]

Crystal structures of nNOS with both lead compounds **1** and **2** have been solved.[18] As shown in Figure 1B, the aminopyridine moiety of **1** binds to the heme, leaving the *m*-fluorophenyl tail extending into a peripheral pocket (Tyr[706], Leu[337], and Met[336]) at the edge of the active site.[18] This was the predicted binding mode. The aminopyridine of **1** was designed to replace the

Received: August 17, 2010
Published: March 16, 2011

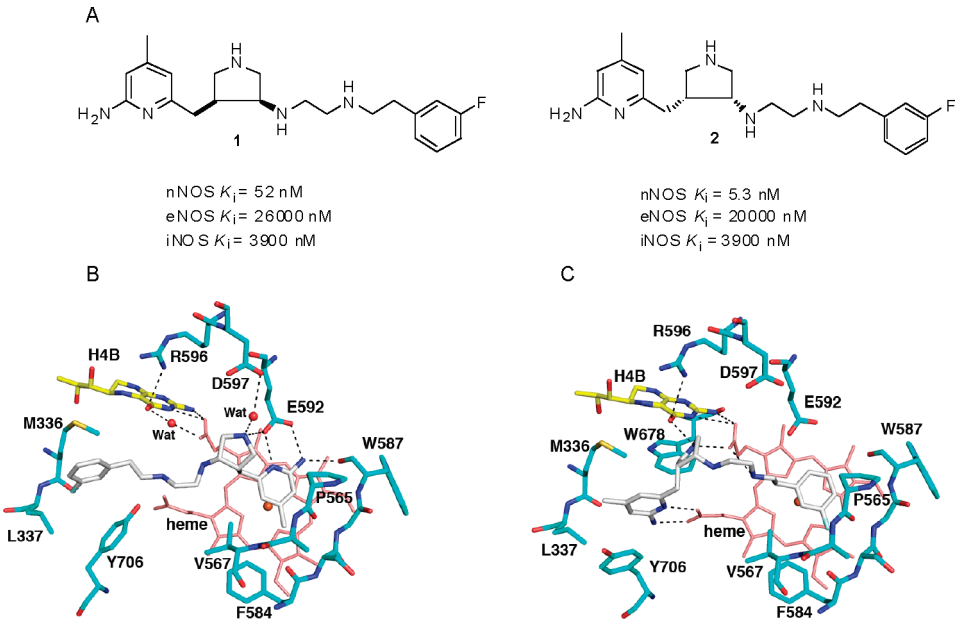

Figure 1. (A) Chemical structures and inhibitory activities of **1** and **2**. (B, C) View of the active site of nNOS complexed with inhibitor **1** (gray) (B) and **2** (gray) (C), showing also heme (pink), tetrahydrobiopterin (H_4B, yellow), and key residues (cyan) in the active site.

guanidinium group of the substrate, L-arginine, which ion-pairs with Glu[592] or its homologue in all NOS isoforms. The pyrrolidine nitrogen of **1** replaces the interaction between the α-amino group of L-arginine, which extends up to and interacts with Asp[597]. Inhibitor **1** therefore mimics many of the interactions between active site groups and L-arginine. The main reason that **1** is selective for nNOS is that the residue in eNOS that corresponds to Asp[597] in nNOS is an Asn, and thus, there is greater electrostatic stabilization between the positive charge on the pyrrolidine N atom of the inhibitor and the electronegative environment created by both Asp[597] and Glu[592] in nNOS. Interestingly, however, inhibitor **2** binds to the active site of nNOS employing a totally different binding mode, the "flipped" binding mode (Figure 1C); the aminopyridine binds in the peripheral pocket (Tyr[706], Leu[337], and Met[336]) and makes hydrogen bonds with a heme propionate, while the *m*-fluorophenyl moiety sits above the heme.[18] The fact that the aminopyridine moiety can bind to two different binding sites in the active site of nNOS by virtue of the molecule flipping over provides an intriguing strategy for designing inhibitors for nNOS. We hypothesized that effective inhibition of nNOS could be achieved by double-headed aminopyridine derivatives (**3**, Figure 2) with an optimizable linker. Compared to the "parent compounds" (**1** and **2**), inhibitor **3** possesses attractive advantages. First, the highly polar amino groups in the pyrrolidine core and lipophilic tail of the lead compounds are replaced by a hydrophobic linker. The significant increase in lipophilicity of **3** (Table S1 in Supporting Information), as a consequence, could potentially improve the BBB permeability of the inhibitors, providing a strategy to bypass the difficulty in modifying the chemical structure of compounds **1** and **2**. Moreover, the simplicity of the chemical structure of **3** could significantly increase the efficiency of the synthesis, which is essential for future preclinical and clinical studies.

CHEMISTRY

Inhibitor **3a** was synthesized using a two-step procedure (Scheme 1). *N*-Boc-2-amino-4,6-dimethylpyridine (**4**) was

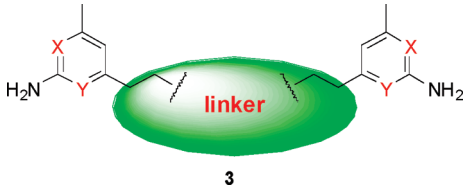

Figure 2. General structure of inhibitor **3**.

treated with NaH, and the resulting anion was allowed to react with bis-bromide **5a** to give **6a** in good yields. Next, the two Boc-protecting groups of **6a** were removed with TFA to generate **3a** in high yields.

The synthesis of **3b**−**d** began with 2,5-dimethylpyrrole-protected 2-amino-4,6-dimethylpyridine (**7**,[23] Scheme 2). The utilization of 2,5-dimethylpyrrole-protecting group has found its application in synthesizing NOS inhibitors.[23,24] Compound **7** was treated with *n*-butyllithium (*n*-BuLi) at −78 °C, followed by the addition of **5a** or **5b** to produce **6b**−**d**. Then the 2,5-dimethylpyrrole protecting groups were removed with hydroxylamine hydrochloride ($NH_2OH \cdot HCl$) at 100 °C to generate **3b**−**d** in excellent yields.

To synthesize inhibitors **3e**−**h**, compound **7** was treated with *n*-BuLi at −78 °C, followed by the addition of **5c** or **5d** to give protected inhibitors **6e**−**h** (Scheme 3). The 2,5-dimethylpyrrole protecting groups of **6e**−**h** were removed with $NH_2OH \cdot HCl$ at 100 °C to generate **3e**−**h** in excellent yields. The synthesis of **3i** is similar to that for **3e**−**h** except **7** was treated with lithium diisopropylamide (LDA) at 0 °C following a reported procedure.[24]

The syntheses of inhibitors **3j**−**n**, with 3,5-bis-substituted pyridine or 2,6-bis-substituted pyridine or 3,5-bis-substituted aniline as the linker, began with **7** (Scheme 4). Compound **7** was treated with *n*-BuLi at −78 °C, and the resulting anion was allowed to react with **5e**, **5f**, or **5g** to give **6j**−**n**.[25] The 2,5-dimethylpyrrole protecting groups of **6j**−**m** were removed with $NH_2OH \cdot HCl$ at 100 °C to generate **3j**−**n** in very good yields.

dx.doi.org/10.1021/jm101071n | *J. Med. Chem.* 2011, 54, 2039–2048

Scheme 1. Synthesis of 3a[a]

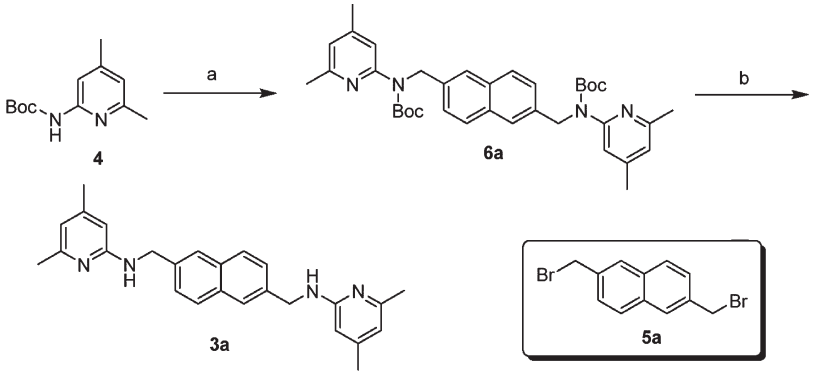

[a] Reagents and conditions: (a) (i) NaH, 0 °C, 15 min, (ii) **5a**, 6 h, 81%; (b) TFA/CH_2Cl_2 (1:1), room temp, 8 h, 90%.

Scheme 2. Synthesis of 3b−d[a]

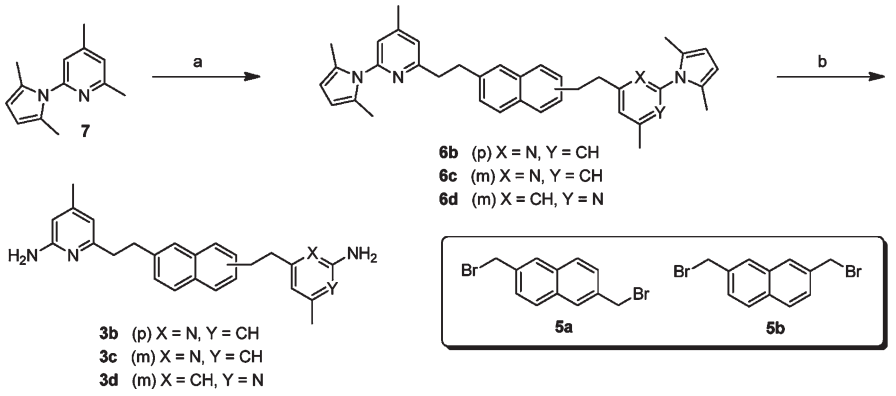

[a] Reagents and conditions: (a) (i) *n*-BuLi, −78 to 0 °C, 30 min, (ii) **5a** or **5b**; (b) $NH_2OH \cdot HCl$, EtOH/H_2O (2:1), 100 °C, 20 h, 90−92%.

Scheme 3. Synthesis of 3e−h[a]

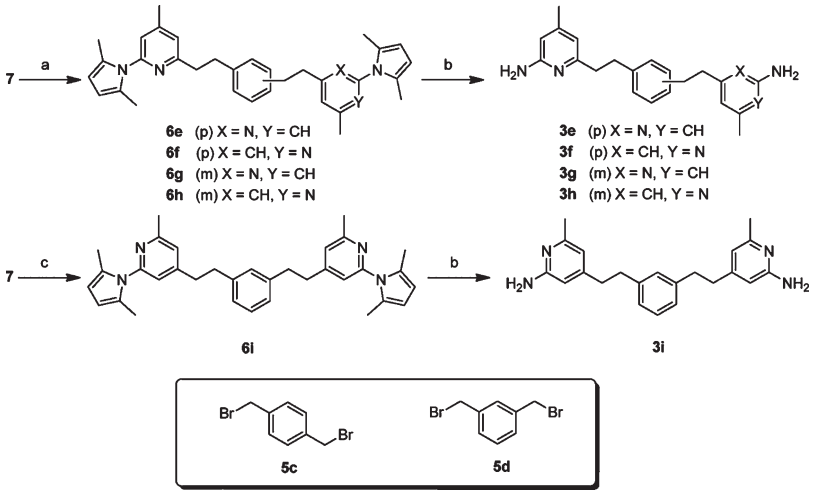

[a] Reagents and conditions: (a) (i) *n*-BuLi, −78 to 0 °C, 30 min, (ii) **5c** or **5d**; (b) $NH_2OH \cdot HCl$, EtOH/H_2O (2:1), 100 °C, 20 h, 85−90%; (c) (i) LDA, 0 °C, 30 min, (ii) **5d**, 65%.

RESULTS AND DISCUSSION

The inhibition constants (K_i) of these compounds were determined for all three NOS isoforms using the oxyhemoglobin NO capture assay,[26] as summarized in Table 1. The compounds with a naphthalene linker, **3a−d**, were tested against nNOS because the length of these compounds is similar to those of the

dx.doi.org/10.1021/jm101071n |*J. Med. Chem.* 2011, 54, 2039–2048

Scheme 4. Synthesis of 3j−n[a]

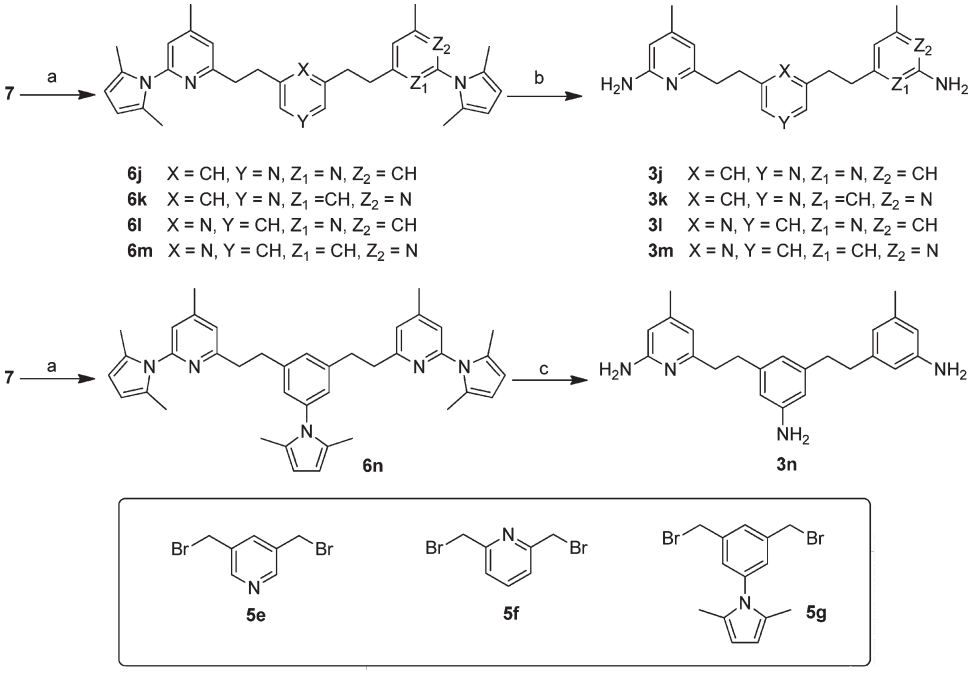

[a] Reagents and conditions: (a) (i) *n*-BuLi, −78 to 0 °C, 30 min, (ii) **5e**, **5f**, or **5g**; (b) $NH_2OH \cdot HCl$, $EtOH/H_2O$ (2:1), 100 °C, 20 h, 80−88%; (c) $NH_2OH \cdot HCl$, $EtOH/H_2O$ (2:1), 100 °C, 36 h, 85%.

parent aminopyridine-pyrrolidine inhibitors (Figure 1, **1** and **2**). Compound **3a**, an internal amidine dimer, showed poor binding, whereas the compounds with the external amidine functionality, **3b** and **3c**, exhibited submicromolar binding affinity to nNOS and modest selectivity against eNOS and iNOS. However, the asymmetric dimer, **3d**, was a poor inhibitor. Compounds **3e−i**, having a shorter 1,3- or 1,4-bis-substituted benzene linker between the two aminopyridine head groups, showed improved potency by 5- to 10-fold. Again, the orientation of the amidine functionality was important. Compound **3i** binds rather poorly to nNOS when the methyl group is next to the ring nitrogen in both aminopyridine groups. To further improve inhibitor potency and selectivity, we sought to modify the 1,3-bis-substituted benzene by additional heteroatoms. Compounds **3j−n** were synthesized with a pyridine linker, and **3n** was synthesized with an aniline linker. The best inhibitor in this series, **3j**, showed better potency (25 nM) than its phenyl analogue **3g** (49 nM), with a 107-fold selectivity for nNOS over eNOS.

We have also determined the crystal structures of several of these inhibitors complexed to both nNOS and eNOS;[27] however, we confine the present discussion to the most potent inhibitor, **3j**. Compound **3j** binds as designed with one aminopyridine interacting with Glu^{592} and the second extending out of the active site, where it interacts with the heme propionate. However, in nNOS a second **3j** molecule (**3jB**) also binds (Figure 3). NOS is a homodimer, and the H_4B cofactor binds at the dimer interface, where it interacts with both subunits A and B of the dimer. One aminopyridine of **3jB** displaces the H_4B cofactor. This places the bridging pyridine of **3jB** in position to coordinate a new Zn^{2+} ion along with Asp^{600}, a chloride ion, and His^{692}(B) of subunit B at the dimer interface. For this to occur, Arg^{596} must move from its position where it normally interacts with H_4B. The new position of Arg^{596} enables its interactions with Asp^{597} and Glu^{592}. In order for His^{692}(B) to coordinate to the Zn^{2+} ion, there must be a slight tightening of the dimer interface and His^{692} (B) must adopt a new rotomer conformation. None of this occurs in eNOS, and only one **3j** molecule binds in the active site as initially predicted. On the basis of an extensive mutagenesis analysis,[27] we concluded that the enhanced stability of the dimer in eNOS compared to nNOS prevents the motions required to coordinate the Zn^{2+} ion in eNOS, thereby preventing the binding of **3jB**.

Binding of only one **3j** in eNOS compared to the binding of two molecules of **3j** and displacement of H_4B in nNOS may account for the 107-fold selectivity of this inhibitor for nNOS over eNOS. However, this modest isoform selectivity implies that the inhibitory potency is likely dominated by the binding of the first **3j** that occupies the substrate binding site, which occurs in both nNOS and eNOS. The binding of a second **3jB** in nNOS and displacement of H_4B enhance the potency to nNOS about 100-fold over eNOS. Despite the modest selectivity, the identification of a second binding pocket in nNOS that requires substantial structural changes that do not take place in eNOS provides a new window of opportunity for the design of novel nNOS-selective inhibitors. Inhibitor **3j** can serve as a NOS active site recognizing building block for developing other inhibitors that can further explore the subtle differences in the active site of nNOS and eNOS, which the good isoform selectivity of the parental inhibitors, **1** and **2**, was based on.[18]

The activities of the best compounds, **3g**, **3h**, **3j**, and **3k**, were further tested in a cell-based assay, in direct comparison with lead compound **2**.[28] Inhibitors **3g** and **3h**, as well as lead **2**, showed almost no activity in the cell-based assay, suggesting that these compounds are blocked by the cellular membrane (Figure 4). Inhibitors **3j** and **3k**, however, showed good membrane penetration ability. The best compound, **3j**, has an IC_{50} value in the

dx.doi.org/10.1021/jm101071n |*J. Med. Chem.* 2011, 54, 2039–2048

Table 1. K_i [a] Values and Selectivity of 3a−n

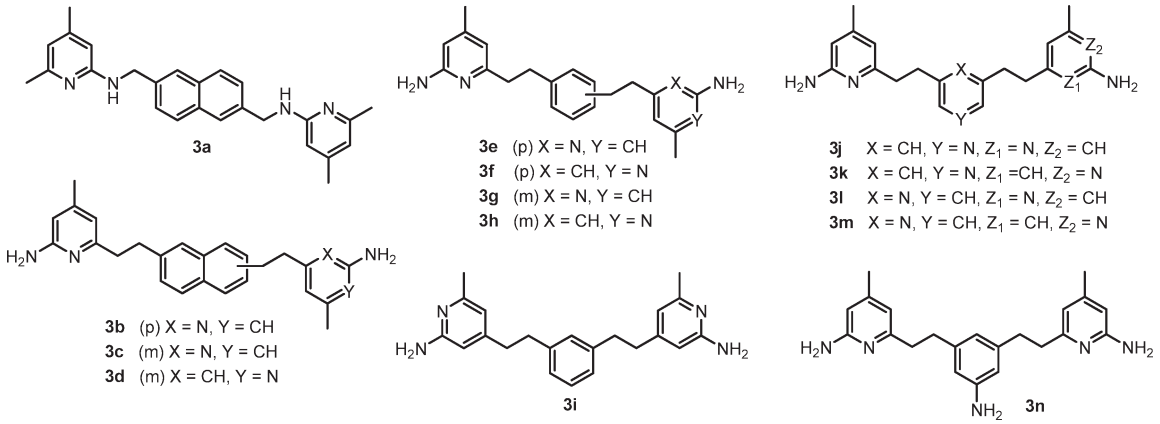

inhibitor	nNOS (nM)	eNOS (nM)	iNOS (nM)	n/e [b]	n/i [b]
3a	>1000	ND[c]	ND[c]	ND[c]	ND[c]
3b	241	1740	2270	7.22	9.42
3c	102	1520	2050	14.9	20.1
3d	>1000	ND[c]	ND[c]	ND[c]	ND[c]
3e	97	2390	2410	24.6	24.8
3f	167	ND[c]	ND[c]	ND[c]	ND[c]
3g	49	1410	682	28.8	13.9
3h	38	4200	2730	111	71.8
3i	>1000	ND[c]	ND[c]	ND[c]	ND[c]
3j	25	2680	1450	107	58
3k	103	16100	1910	156	19
3l	99	9400	4750	95	48
3m	195	20000	12600	102	64
3n	85	4950	3400	58	40

[a] The K_i values were calculated based on the directly measured IC_{50} values, which represent at least duplicate measurements with standard deviations of ±10%. [b] The ratio of K_i(eNOS or iNOS) to K_i(nNOS). [c] Not determined.

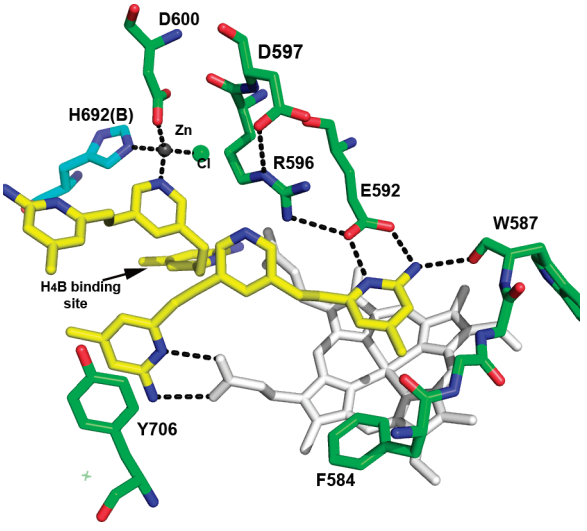

Figure 3. Crystal structure of nNOS complexed with **3j**.[27] Major hydrogen bonds and the ligation bonds of zinc ion are depicted with dashed lines. The native H_4B binding site that is occupied by **3jB** is labeled.

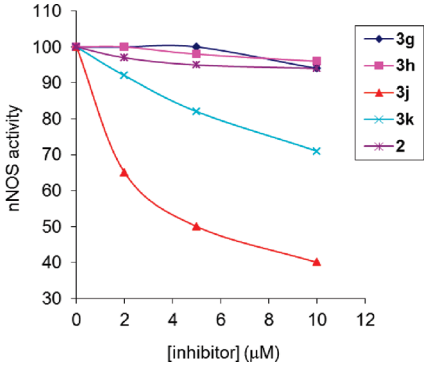

Figure 4. Inhibition of nNOS in 293T cells overexpressing nNOS (293T/nNOS cells). 293T/nNOS cells were treated with A23187 (5 μM) and various concentrations of inhibitors **2** and **3g**−**k**. After 8 h, the amount of nitrite in culture medium was quantified with the Griess reagent. Each data point is an average of two independent experiments.

cell-based assay of 5 μM, which is significantly better than that of lead compound **2**, which, we believe, is due to the result of its increased lipophilicity (Table S1). Compared to its in vitro

dx.doi.org/10.1021/jm101071n |J. Med. Chem. 2011, 54, 2039–2048

activity, the potency of **3j** in the cell-based assay is weaker, which may be the result of its affinity for one of the active efflux transporters (e.g., *p*-glycoprotein)[29−32] or may just represent the K_d for membrane transport and not K_i nNOS inhibition. These results indicate that double-headed scaffold **3** is a promising candidate for future development of bioavailable nNOS inhibitors.

SUMMARY

Double-headed aminopyridine inhibitors (**3a**−**m**) were designed based on the unexpected binding mode of chiral pyrrolidine leads **1** and **2**[18] and synthesized as a novel class of inhibitors for nNOS. Inhibitor **3j**, the best inhibitor discovered from the series, exhibits high potency and modest selectivity for nNOS. It showed improved membrane permeability based on a cell-based assay. The simplicity of the chemical structures of **3a**−**n** makes the synthesis of the new class of inhibitors much more efficient than the lead compounds (**1** and **2**). The crystal structure of the nNOS−**3j** complex also revealed an unexpected second binding site unique to nNOS and illustrated the importance of the substrate and H_4B binding sites in inhibitor development. This new binding site also provides the basis for the design of novel and isoform-selective inhibitors.

EXPERIMENTAL SECTION

All experiments were conducted under anhydrous conditions in an atmosphere of argon using flame-dried apparatus and employing standard techniques in handling air-sensitive materials. All solvents were distilled and stored under an argon or nitrogen atmosphere before use. All reagents were used as received. Aqueous solutions of sodium bicarbonate, sodium chloride (brine), and ammonium chloride were saturated. Analytical thin layer chromatography was visualized by ultraviolet light. Flash column chromatography was carried out under a positive pressure of nitrogen. ^{1}H NMR spectra were recorded on 500 MHz spectrometers. Data are presented as follows: chemical shift (in ppm on the δ scale relative to δ = 0.00 ppm for the protons in tetramethylsilane (TMS)), integration, multiplicity (s = singlet, d = doublet, t = triplet, q = quartet, m = multiplet, br = broad), coupling constant (J/Hz). Coupling constants were taken directly from the spectra and are uncorrected. ^{13}C NMR spectra were recorded at 125 MHz, and all chemical shift values are reported in ppm on the δ scale with an internal reference of δ 77.0 or 49.0 for $CDCl_3$ or MeOD, respectively. High-resolution mass spectra were measured by liquid chromatography/time-of-flight mass spectrometry (LC-TOF). The purity of the tested compounds was determined by elemental analysis and was >95%.

General Method A: Synthesis of 2,5-Dimethylpyrrole-Protected Inhibitors 6b−m. To a solution of **7** (500 mg, 2.5 mmol) in THF (10 mL) at −78 °C was added *n*-BuLi (1.6 M solution in hexanes, 1.64 mL, 2.63 mmol) dropwise. The resulting dark red solution after the addition was transferred to an ice bath. After 30 min, a solution of bromide **5a**, **5b**, **5c**,[20] or **5d**[20] (1 M in THF) was added dropwise until the dark red color disappeared. The reaction mixture was allowed to stir at 0 °C for an additional 10 min and then quenched with H_2O (20 μL). The solvent was removed by rotary evaporation, and the resulting yellow oil was purified by flash chromatography (EtOAc/hexanes) to yield 2,5-dimethylpyrrole-protected inhibitors **6b**−**m**.

General Method B: Synthesis of Inhibitors 3a−m. To a solution of **6a**−**m** (0.5 mmol) in EtOH (10 mL) was added hydroxylamine hydrochloride ($NH_2OH\cdot HCl$, 340 mg, 5 mmol) followed by H_2O (5 mL). The reaction mixture was heated at 100 °C for 20 h. After cooling to room temperature, the reaction mixture was partitioned between Et_2O (50 mL) and 2 N NaOH (25 mL). The aqueous layer was extracted with Et_2O (2 × 25 mL), and the combined organic layers were dried over Na_2SO_4. The solvent was removed by rotary evaporation, and the resulting yellow oil was purified by flash chromatography (5−10% MeOH in CH_2Cl_2) to yield inhibitors **6a**−**m**.

Di-*tert*-butyl Naphthalene-2,6-diylbis(methylene)bis(4,6-dimethylpyridin-2-ylcarbamate) (6a). To a solution of **4** (444 mg, 2 mmol) in dimethylformamide (DMF, 10 mL) at 0 °C was added NaH (60% in mineral oil, 88 mg, 2.2 mmol). After 15 min, bis-bromide **5a** (314 mg, 1 mmol) was added slowly. The reaction mixture was allowed to stir at room temperature for 6 h and then concentrated. The crude product was purified by flash column chromatography (EtOAc/hexanes, 1:9 to 1:4) to yield **6a** (960 mg, 81%) as a white solid: ^{1}H NMR (500 MHz, $CDCl_3$) δ 1.41 (s, 18H), 2.29 (s, 6H), 2.45 (s, 6H), 5.33 (s, 4H), 6.72 (s, 2H), 7.28 (s, 2H), 7.42−7.44 (d, J = 8.5, 2H), 7.68−7.70 (m, 4H); ^{13}C NMR (125 MHz, $CDCl_3$) δ 14.4, 21.3, 24.4, 28.5, 31.9, 50.5, 81.2, 117.7, 120.6, 126.1, 126.3, 127.8, 132.6, 137.1, 148.7, 154.0, 154.7, 156.5; LC-TOF (M + H^+) calcd for $C_{36}H_{45}N_4O_4$ 597.344 08, found 597.344 92.

2,6-Bis(2-(6-(2,5-dimethyl-1*H*-pyrrol-1-yl)-4-methylpyridin-2-yl)ethyl)naphthalene (6b). Compound **6b** was synthesized starting with **7** and **5a** using general method A (60%): ^{1}H NMR (500 MHz, $CDCl_3$) δ 2.18 (s, 12H), 2.39 (s, 6H), 3.20−3.40 (m, 8H), 5.94 (s, 4H), 6.90 (s, 2H), 6.97 (s, 2H), 7.34−7.36 (d, J = 8.5 Hz, 2H), 7.61 (s, 2H), 7.69−7.71 (d, J = 8.5 Hz, 2H); ^{13}C NMR (125 MHz, $CDCl_3$) δ 13.5, 21.3, 36.2, 39.9, 107.0, 120.4, 122.9, 126.6, 127.6, 127.7, 128.8, 132.5, 138.6, 149.7, 151.9, 161.2; LC-TOF (M + H^+) calcd for $C_{38}H_{41}N_4$ 553.333 12, found 553.333 82.

2,7-Bis(2-(6-(2,5-dimethyl-1*H*-pyrrol-1-yl)-4-methylpyridin-2-yl)ethyl)naphthalene (6c). Compound **6c** was synthesized starting with **7** and **5b** using general method A (55%): ^{1}H NMR (500 MHz, $CDCl_3$) δ 2.18 (s, 12H), 2.39 (s, 6H), 3.15−3.25 (m, 8H), 5.94 (s, 4H), 6.90 (s, 2H), 6.98 (s, 2H), 7.32−7.34 (d, J = 8.5 Hz, 2H), 7.57 (s, 2H), 7.75−7.76 (d, J = 8.5 Hz, 2H); ^{13}C NMR (125 MHz, $CDCl_3$) δ 13.5, 21.3, 36.3, 39.9, 107.0, 120.4, 122.9, 126.4, 126.9, 127.9, 128.8, 130.9, 134.1, 139.4, 149.7, 151.9, 161.2; LC-TOF (M + H^+) calcd for $C_{38}H_{41}N_4$ 553.333 12, found 553.333 79.

2-(2,5-Dimethyl-1*H*-pyrrol-1-yl)-4-(2-(7-(2-(6-(2,5-dimethyl-1*H*-pyrrol-1-yl)-4-methylpyridin-2-yl)ethyl)naphthalen-2-yl)ethyl)-6-methylpyridine (6d). Compound **6d** was synthesized starting with **7** and **5b** using general method A (35%): ^{1}H NMR (500 MHz, $CDCl_3$) δ 2.02 (s, 6H), 2.16 (s, 6H), 2.36 (s, 3H), 2.57 (s, 3H), 3.00−3.15 (m, 4H), 3.15−3.30 (m, 4H), 5.86 (s, 2H), 5.93 (s, 2H), 6.79 (s, 1H), 6.88 (s, 1H), 6.96 (s, 1H), 7.03 (s, 1H), 7.25−7.27 (d, J = 10 Hz, 1H), 7.31−7.33 (d, J = 10 Hz, 1H), 7.47 (s, 1H), 7.54 (s, 1H), 7.73−7.74 (d, J = 9.0 Hz, 2H); ^{13}C NMR (125 MHz, $CDCl_3$) δ 13.2, 13.5, 21.2, 24.5, 36.2, 36.98, 37.02, 39.9, 106.8, 107.0, 119.5, 120.4, 122.5, 122.9, 126.4, 126.5, 126.6, 127.2, 127.9, 128.1, 128.6, 128.7, 131.0, 134.0, 138.2, 139.6, 149.8, 151.7, 151.9, 153.1, 158.5, 161.1; LC-TOF (M + H^+) calcd for $C_{38}H_{41}N_4$ 553.333 12, found 553.332 96.

1,4-Bis(2-(6-(2,5-dimethyl-1*H*-pyrrol-1-yl)-4-methylpyridin-2-yl)ethyl)benzene (6e). Compound **6e** was synthesized starting with **7** and **5c** using general method A (65%): ^{1}H NMR (500 MHz, $CDCl_3$) δ 2.21 (s, 12H), 2.44 (s, 6H), 3.12−3.15 (m, 8H), 5.97 (s, 4H), 6.94 (s, 2H), 7.01 (s, 2H), 7.18 (s, 4H); ^{13}C NMR (125 MHz, $CDCl_3$) δ 13.6, 21.3, 35.8, 40.1, 107.0, 120.3, 122.9, 128.8, 139.4, 149.7, 151.9, 161.4; LC-TOF (M + H^+) calcd for $C_{34}H_{39}N_4$ 503.317 47, found 503.318 28.

2-(2,5-Dimethyl-1*H*-pyrrol-1-yl)-4-(4-(2-(6-(2,5-dimethyl-1*H*-pyrrol-1-yl)-4-methylpyridin-2-yl)ethyl)phenethyl)-6-methylpyridine (6f). Compound **6f** was synthesized starting with **7** and **5c** using general method A (35%): ^{1}H NMR (500 MHz, $CDCl_3$) δ 2.12 (s, 6H), 2.19 (s, 6H), 2.43 (s, 3H), 2.61 (s, 3H), 2.99 (s, 4H), 3.05−3.20 (s, 4H), 5.91 (s, 2H), 5.95 (s, 2H), 6.83 (s, 1H), 6.92 (s, 1H), 6.99 (s, 1H), 7.04 (s, 1H), 7.10−7.12 (d, J = 8.0 Hz, 2H), 7.16−7.18 (d, J = 7.5, 2H); ^{13}C NMR (125 MHz, $CDCl_3$) δ 13.4, 13.5, 21.3, 24.5, 35.7,

36.4, 37.2, 40.1, 106.9, 107.0, 119.5, 120.3, 122.5, 122.8, 128.67, 128.70, 128.73, 128.9, 138.3, 139.8, 149.7, 151.7, 151.9, 153.3, 158.5, 161.3; LC-TOF ($M + H^+$) calcd for $C_{34}H_{39}N_4$ 503.317 47, found 503.318 45.

1,3-Bis(2-(6-(2,5-dimethyl-1*H*-pyrrol-1-yl)-4-methylpyridin-2-yl)ethyl)benzene (6g). Compound **6g** was synthesized starting with **7** and **5d** using general method A (60%): ^{1}H NMR (500 MHz, $CDCl_3$) δ 2.19 (s, 12H), 2.42 (s, 6H), 3.00−3.20 (m, 8H), 5.94 (s, 4H), 6.91 (s, 2H), 6.97 (s, 2H), 7.06−7.08 (m, 3H), 7.21−7.23 (m, 1H); ^{13}C NMR (125 MHz, $CDCl_3$) δ 13.5, 21.7, 36.2, 40.1, 107.0, 120.3, 122.9, 126.4, 128.68, 128.74, 129.0, 141.9, 149.7, 151.9, 161.3; LC-TOF ($M + H^+$) calcd for $C_{34}H_{39}N_4$ 503.317 47, found 503.318 14.

2-(2,5-Dimethyl-1*H*-pyrrol-1-yl)-4-(3-(2-(6-(2,5-dimethyl-1*H*-pyrrol-1-yl)-4-methylpyridin-2-yl)ethyl)phenethyl)-6-methylpyridine (6h). Compound **6h** was synthesized starting with **7** and **5d** using general method A (35%): ^{1}H NMR (500 MHz, $CDCl_3$) δ 2.12 (s, 6H), 2.19 (s, 6H), 2.41 (s, 3H), 2.60 (s, 3H), 2.97 (s, 4H), 3.05−3.20 (m, 4H), 5.91 (s, 2H), 5.94 (s, 2H), 6.83 (s, 1H), 6.91 (s, 1H), 6.97 (s, 1H), 7.02 (s, 1H), 7.05−7.15 (m, 3H), 7.21−7.25 (m, 1H); ^{13}C NMR (125 MHz, $CDCl_3$) δ 13.4, 13.5, 21.2, 24.5, 36.1, 36.8, 37.2, 40.1, 106.9, 107.0, 119.4, 120.3, 122.5, 122.8, 126.3, 126.7, 128.65, 128.71, 128.8, 128.9, 140.8, 142.1, 149.8, 151.7, 151.9, 153.2, 158.5, 161.2; LC-TOF ($M + H^+$) calcd for $C_{34}H_{39}N_4$ 503.317 47, found 503.318 40.

1,3-Bis(2-(2-(2,5-dimethyl-1*H*-pyrrol-1-yl)-6-methylpyridin-4-yl)ethyl)benzene (6i). To a solution of **7** (500 mg, 2.5 mmol) in THF (10 mL) at 0 °C was added lithium diisopropylamide (2.0 M solution in THF, 1.32 mL, 2.63 mmol) dropwise. The resulting dark red solution after the addition was allowed to warm to room temperature. After 30 min, a solution of bromide **5d** (1 M in THF) was added dropwise until the dark red color disappeared. The reaction mixture was allowed to stir at 0 °C for an additional 10 min and then quenched with H_2O (20 μL). The solvent was removed by rotary evaporation, and the resulting yellow oil was purified by flash chromatography (EtOAc/hexanes, 1:9) to yield 2,5-dimethylpyrrole-protected inhibitors **6i** (405 mg, 65%): ^{1}H NMR (500 MHz, $CDCl_3$) δ 2.09 (s, 12H), 2.56 (s, 6H), 2.94 (s, 6H), 5.88 (s, 3H), 6.81 (s, 1H), 6.95−7.05 (m, 4H), 7.20−7.23 (m, 1H); ^{13}C NMR (125 MHz, $CDCl_3$) δ 13.4, 24.5, 36.7, 37.1, 106.9, 119.3, 122.4, 126.6, 128.6, 128.8, 141.0, 151.8, 153.1, 158.5; LC-TOF ($M + H^+$) calcd for $C_{34}H_{39}N_4$ 503.317 47, found 503.318 01.

3,5-Bis(bromomethyl)pyridine (5e). To pyridine-3,5-diyldimethanol (2 g, 14 mmol) was added 60% HBr (15 mL) slowly. The mixture was heated at 125 °C for 6 h and then cooled to room temperature. The resulting residue was dissolved in H_2O (50 mL) to give a yellow solution. To this solution was added saturated $NaHCO_3$ to pH 8. The resulting aqueous solution was extracted with CH_2Cl_2 (4 × 50 mL), and the combined organic layers were dried over Na_2SO_4. The solvent was removed by rotary evaporation, and the resulting material was purified by flash column chromatography (EtOAc/hexanes, 1:4) to yield 3,5-bis(bromomethyl)pyridine (**5e**, 3.5 g, 95%) as a white solid: ^{1}H NMR (500 MHz, $CDCl_3$) δ 4.45 (s, 4H), 7.74−7.75 (t, J = 2.0 Hz, 1H), 8.53−8.54 (d, J = 2.0 Hz, 2H); ^{13}C NMR (125 MHz, $CDCl_3$) δ 29.3, 134.0, 137.3, 149.8; LC-TOF ($M + H^+$) calcd for $C_7H_8Br_2N$ 263.902 35, found 263.901 82.

3,5-Bis(2-(6-(2,5-dimethyl-1*H*-pyrrol-1-yl)-4-methylpyridin-2-yl)ethyl)pyridine (6j). Compound **6j** was synthesized starting with **7** and **5e** using general method A (55%): ^{1}H NMR (500 MHz, $CDCl_3$) δ 2.13 (s, 12H), 2.38 (s, 6H), 3.05 (s, 8H), 5.90 (s, 4H), 6.88 (s, 2H), 6.91 (s, 2H), 7.34 (s, 1H), 8.21−8.22 (d, J = 2.5 Hz, 2H); ^{13}C NMR (125 MHz, $CDCl_3$) δ 13.5, 21.2, 32.8, 39.4, 107.0, 120.5, 122.9, 128.6, 136.2, 136.5, 147.9, 149.8, 152.0, 160.3; LC-TOF ($M + H^+$) calcd for $C_{33}H_{38}N_5$ 504.312 72, found 504.312 65.

2-(2,5-Dimethyl-1*H*-pyrrol-1-yl)-4-(2-(5-(2-(6-(2,5-dimethyl-1*H*-pyrrol-1-yl)-4-methylpyridin-2-yl)ethyl)pyridin-3yl)ethyl)-6-methylpyridine (6k). Compound **6k** was synthesized starting with **7** and **5e** using general method A (30%): ^{1}H NMR (500 MHz, $CDCl_3$) δ 2.08 (s, 6H), 2.13 (s, 6H), 2.38 (s, 3H), 2.56 (s, 3H), 2.94 (s, 4H), 3.06 (s, 4H), 5.88 (s, 2H), 5.91 (s, 2H), 6.80 (s, 1H), 6.89 (s, 1H), 6.92 (s, 1H), 6.97 (s, 1H), 7.31 (s, 1H), 8.25 (s, 1H), 8.29 (s, 1H); ^{13}C NMR (125 MHz, $CDCl_3$) δ 13.4, 13.5, 21.2, 24.5, 32.8, 33.8, 36.7, 39.4, 107.0, 119.2, 120.6, 122.3, 122.9, 128.60, 128.66, 128.69, 135.6, 136.2, 136.8, 149.88, 149.93, 151.9, 152.0, 152.3, 158.8, 160.3; LC-TOF ($M + H^+$) calcd for $C_{33}H_{38}N_5$ 504.312 72, found 504.312 36.

2,6-Bis(bromomethyl)pyridine (5f). To pyridine-2,6-diyldimethanol (2 g, 14 mmol) was added 60% HBr (15 mL) slowly. The mixture was heated at 125 °C for 6 h and then cooled to room temperature. The resulting residue was dissolved in H_2O (50 mL) to give a yellow solution. To this solution was added saturated $NaHCO_3$ to pH 8. The resulting aqueous solution was extracted with CH_2Cl_2 (4 × 50 mL), and the combined organic layers were dried over Na_2SO_4. The solvent was removed by rotary evaporation, and the resulting material was purified by flash column chromatography (EtOAc/hexanes, 1:9 to 1:4) to yield 2,6-bis(bromomethyl)pyridine (**5f**, 3.5 g, 96%) as a white solid: ^{1}H NMR (500 MHz, $CDCl_3$) δ 4.53 (s, 4H), 7.36−7.38 (d, J = 8.0 Hz, 2H), 7.68−7.71 (dd, J = 7.5, 8.0 Hz, 1H); ^{13}C NMR (125 MHz, $CDCl_3$) δ 33.8, 123.1, 138.4, 157.0; LC-TOF ($M + H^+$) calcd for $C_7H_8Br_2N$ 263.902 35, found 263.901 93.

2,6-Bis(2-(6-(2,5-dimethyl-1*H*-pyrrol-1-yl)-4-methylpyridin-2-yl)ethyl)pyridine (6l). Compound **6l** was synthesized starting with **7** and **5f** using general method A (58%): ^{1}H NMR (500 MHz, $CDCl_3$) δ 2.08 (s, 12H), 2.37 (s, 6H), 3.25 (s, 8H), 5.91 (s, 4H), 6.85−6.87 (d, J = 9.5 Hz, 2H), 6.93−6.95 (d, J = 7.5 Hz, 2H), 7.00 (s, 2H), 7.42−7.46 (dd, J = 7.5, 8.0 Hz, 1H); ^{13}C NMR (125 MHz, $CDCl_3$) δ 13.5, 21.2, 37.9, 38.1, 106.9, 120.2, 120.5, 122.9, 128.7, 136.7, 149.6, 151.8, 160.8, 161.3; LC-TOF ($M + H^+$) calcd for $C_{33}H_{38}N_5$ 504.312 72, found 504.312 62.

2-(2,5-Dimethyl-1*H*-pyrrol-1-yl)-4-(2-(6-(2-(6-(2,5-dimethyl-1*H*-pyrrol-1-yl)-4-methylpyridin-2-yl)ethyl)pyridin-2-yl)ethyl)-6-methylpyridine (6m). Compound **6m** was synthesized starting with **7** and **6f** using general method A (37%): ^{1}H NMR (500 MHz, $CDCl_3$) δ 2.07 (s, 6H), 2.11 (s, 6H), 2.37 (s, 3H), 2.55 (s, 3H), 3.10−3.12 (t, J = 3.0 Hz, 4H), 3.21−3.23 (t, J = 3.0 Hz, 4H), 5.87 (s, 2H), 5.90 (s, 2H), 6.80−7.10 (m, 6H), 7.40−7.50 (m, 1H); ^{13}C NMR (125 MHz, $CDCl_3$) δ 13.3, 13.5, 21.2, 24.4, 34.98, 35.041, 37.9, 38.08, 38.15, 38.8, 106.9, 119.3, 120.3, 120.5, 120.8, 122.4, 122.8, 122.9, 128.6, 128.7, 136.9, 149.6, 151.8, 153.2, 153.3, 158.4, 159.7, 160.8, 161.1, 161.3; LC-TOF ($M + H^+$) calcd for $C_{33}H_{38}N_5$ 504.312 72, found 504.312 26.

16,6′-(2,2′-(5-(2,5-Dimethyl-1*H*-pyrrol-1-yl)-1,3phenylene)bis(ethane-2,1-diyl))bis(2-(2,5-dimethyl-1*H*-pyrrol-1-yl)-4-methylpyridine) (6n). Compound **6n** was synthesized starting with **7** and **5g** using general method A (55%): ^{1}H NMR (500 MHz, $CDCl_3$) δ 1.94 (s, 6H), 2.11 (s, 12H), 2.35 (s, 6H), 3.07 (s, 8H), 5.85 (s, 2H), 5.88 (s, 4H), 6.81−6.82 (d, J = 1.5 Hz, 2H), 6.85 (s, 2H), 6.87 (s, 2H), 7.06 (s, 1H); ^{13}C NMR (125 MHz, $CDCl_3$) δ 13.0, 13.3, 21.0, 35.3, 39.4, 105.5, 106.6, 106.7, 120.1, 122.6, 125.7, 128.0, 128.4, 128.5, 138.9, 142.5, 149.4, 151.7, 160.5; LC-TOF ($M + H^+$) calcd for $C_{40}H_{46}N_5$ 596.375 32, found 596.375 19.

***N*,*N*′-(Naphthalene-2,6-diylbis(methylene))bis(4,6-dimethylpyridin-2-amine) (3a).** To a solution of **6a** (590 mg, 1.0 mmol) in CH_2Cl_2 (8 mL) was added trifluoroacetic acid (TFA, 8 mL). The reaction mixture was allowed to stir at room temperature for 8 h and then was concentrated. The crude product was purified by flash column chromatography (2−5% MeOH in CH_2Cl_2) to yield **3a** (355 mg, 90%) as a white solid: ^{1}H NMR (500 MHz, $CD_3OD/CDCl_3$) δ 2.28 (s, 6H), 2.48 (s, 6H), 4.60 (s, 4H), 6.46 (s, 4H), 7.45−7.47 (d, J = 8.5, 2H), 7.78 (s, 2H), 7.84−7.86 (d, J = 8.5, 2H); ^{13}C NMR (125 MHz, $CD_3OD/CDCl_3$) δ 18.6, 22.0, 45.9, 106.8, 114.5, 125.6, 129.0, 133.1, 134.3, 147.6, 153.8, 158.0; LC-TOF ($M + H^+$) calcd for $C_{26}H_{29}N_4$ 397.239 22, found 397.239 99.

6,6′-(2,2′-(Naphthalene-2,6-diyl)bis(ethane-2,1-diyl))bis(4-methylpyridin-2-amine) (3b). Inhibitor **3b** was synthesized using general method B (90%): ^{1}H NMR (500 MHz, $CDCl_3$) δ 2.19 (s, 6H), 2.94−2.98 (dd, J = 7.5, 10.5 Hz, 4H), 3.12−3.16 (dd, J = 6.0, 9.0 Hz, 4H), 4.52 (br s, 4H), 6.20 (s, 2H), 6.37 (s, 2H), 7.35−7.36 (d, J = 8.5 Hz, 2H), 7.64 (s, 2H), 7.70−7.72 (d, J = 8.5 Hz, 2H); ^{13}C NMR (125 MHz, $CDCl_3$) δ 21.2, 36.4, 40.0, 106.9, 115.7, 126.4, 127.6, 132.4, 139.0, 149.6, 158.5, 159.6; LC-TOF ($M + H^+$) calcd for $C_{26}H_{29}N_4$ 397.239 22, found 397.239 54.

6,6′-(2,2′-(Naphthalene-2,7-diyl)bis(ethane-2,1-diyl))bis(4-methylpyridin-2-amine) (3c). Inhibitor **3c** was synthesized using general method B (90%): ^{1}H NMR (500 MHz, $CDCl_3$) δ 2.18 (s, 6H), 2.95−2.99 (m, 4H), 2.13−2.17 (m, 4H), 4.55 (br s, 4H), 6.18 (s, 2H), 6.38 (s, 2H), 7.32−7.33 (d, J = 8.5 Hz, 2H), 7.60 (s, 2H), 7.72−7.74 (d, J = 8.0 Hz, 2H); ^{13}C NMR (125 MHz, $CDCl_3$) δ 21.2, 36.5, 40.0, 106.8, 114.6, 126.3, 126.9, 127.8, 130.8, 134.1, 139.8, 149.5, 158.6, 159.7; LC-TOF ($M + H^+$) calcd for $C_{26}H_{29}N_4$ 397.239 22, found 397.239 46. Anal. Calcd for $C_{26}H_{28}N_4 \cdot 0.5H_2O$: C, 77.15; H, 7.33; N, 13.58. Found: C, 77.53; H, 7.14; N, 11.72

4-(2-(7-(2-(6-Amino-4-methylpyridin-2-yl)ethyl)naphthalen-2-yl)ethyl)-6-methylpyridin-2-amine (3d). Inhibitor **3d** was synthesized using general method B (92%): ^{1}H NMR (500 MHz, $CDCl_3$) δ 2.19 (s, 3H), 2.37 (s, 3H), 2.82−2.84 (m, 2H), 2.85−2.99 (m, 2H), 3.00−3.03 (m, 2H), 3.14−3.17 (m, 2H), 4.48 (br s, 4H), 6.16 (s, 1H), 6.19 (s, 1H), 6.38 (s, 1H), 6.43 (s, 1H), 7.25−7.27 (d, J = 8.5 Hz, 1H), 7.33−7.35 (d, J = 8.5 Hz, 1H), 7.55 (s, 1H), 7.61 (s, 1H), 7.73−7.75 (d, J = 8.0 Hz, 2H); ^{13}C NMR (125 MHz, $CDCl_3$) δ 21.2, 24.3, 36.4, 36.9, 37.3, 40.0, 105.6, 106.8, 114.2, 114.6, 126.29, 126.32, 126.7, 127.1, 127.8, 127.9, 130.9, 134.0, 139.0, 140.0, 149.4, 153.1, 156.8, 158.4, 158.6, 159.7; LC-TOF ($M + H^+$) calcd for $C_{26}H_{29}N_4$ 397.239 22, found 397.239 70.

6,6′-(2,2′-(1,4-Phenylene)bis(ethane-2,1-diyl))bis(4-methylpyridin-2-amine) (3e). Inhibitor **3e** was synthesized using general method B (85%): ^{1}H NMR (500 MHz, $CDCl_3$) δ 2.20 (s, 6H), 2.85−2.88 (m, 4H), 2.94−2.98 (m, 4H), 4.39 (s, 4H), 6.19 (s, 2H), 6.36 (s, 2H), 7.16 (s, 4H); ^{13}C NMR (125 MHz, $CDCl_3$) δ 21.2, 35.9, 40.2, 106.7, 114.7, 128.6, 139.7, 149.4, 158.4, 160.0; LC-TOF ($M + H^+$) calcd for $C_{22}H_{27}N_4$ 347.223 57, found 347.223 99. Anal. Calcd for $C_{22}H_{26}N_4 \cdot 0.5CH_3OH$: C, 74.55; H, 7.79; N, 15.46. Found: C, 73.68; H, 7.27; N, 15.05.

4-(4-(2-(6-Amino-4-methylpyridin-2-yl)ethyl)phenethyl)-6-methylpyridin-2-amine (3f). Inhibitor **3f** was synthesized using general method B (88%): ^{1}H NMR (500 MHz, $CDCl_3$) δ 2.20 (s, 3H), 2.37 (s, 3H), 2.73−2.76 (m, 2H), 2.83−2.88 (m, 4H), 2.95−2.98 (m, 2H), 4.42 (s, 2H), 4.45 (s, 2H), 6.13 (s, 1H), 6.19 (s, 1H), 6.37 (s, 1H), 6.40 (s, 1H), 7.09−7.19 (d, J = 8.0 Hz, 2H), 7.15−7.17 (d, J = 8.0 Hz, 2H); ^{13}C NMR (125 MHz, $CDCl_3$) δ 21.2, 24.2, 35.9, 36.4, 37.5, 40.2, 105.6, 106.7, 114.3, 114.6, 128.6, 128.7, 138.9, 140.0, 149.5, 153.2, 156.7, 158.3, 158.4, 159.8; LC-TOF ($M + H^+$) calcd for $C_{22}H_{27}N_4$ 347.223 57, found 347.224 10. Anal. Calcd for $C_{22}H_{26}N_4 \cdot 0.5CH_3OH$: C, 74.55; H, 7.79; N, 15.46. Found: C, 73.86; H, 7.37; N, 14.93.

6,6′-(2,2′-(1,3-Phenylene)bis(ethane-2,1-diyl))bis(4-methylpyridin-2-amine) (3g). Inhibitor **3g** was synthesized using general method B (85%): ^{1}H NMR (500 MHz, $CDCl_3$) δ 2.20 (s, 6H), 2.84−2.87 (m, 4H), 2.94−2.98 (m, 4H), 4.44 (br s, 4H), 6.19 (s, 2H), 6.35 (s, 2H), 7.06−7.11 (s, 3H), 7.19−7.22 (m, 1H); ^{13}C NMR (125 MHz, $CDCl_3$) δ 21.2, 36.4, 40.2, 106.7, 114.6, 126.2, 128.5, 129.0, 142.2, 149.4, 158.5, 159.9; LC-TOF ($M + H^+$) calcd for $C_{22}H_{27}N_4$ 347.223 57, found 347.224 02. Anal. Calcd for $C_{22}H_{26}N_4 \cdot 0.5CH_3OH$: C, 74.55; H, 7.79; N, 15.46. Found: C, 73.59; H, 7.62; N, 15.09.

4-(3-(2-(6-Amino-4-methylpyridin-2-yl)ethyl)phenethyl)-6-methylpyridin-2-amine (3h). Inhibitor **3h** was synthesized using general method B (90%): ^{1}H NMR (500 MHz, $CDCl_3$) δ 2.19 (s, 3H), 2.36 (s, 3H), 2.71−2.75 (m, 2H), 2.82−2.87 (m, 4H), 2.95−2.98 (m, 2H), 4.47 (br s, 4H), 6.13 (s, 1H), 6.19 (s, 1H), 6.35 (s, 1H), 6.38 (s, 1H), 6.99−7.01 (d, J = 7.5 Hz, 1H), 7.04 (s, 1H), 7.06−7.08 (d, J = 7.5 Hz, 1H), 7.19−7.22 (m, 1H); ^{13}C NMR (125 MHz, $CDCl_3$) δ 21.2, 24.2, 36.3, 36.8, 37.4, 40.2, 105.6, 106.8, 114.2, 114.6, 126.1, 126.5, 128.6, 128.9, 141.5, 142.3, 149.5, 153.3, 156.6, 158.3, 158.5, 159.7; LC-TOF ($M + H^+$) calcd for $C_{22}H_{27}N_4$ 347.223 57, found 347.224 17. Anal. Calcd for $C_{22}H_{26}N_4 \cdot 0.5CH_3OH$: C, 74.55; H, 7.79; N, 15.46. Found: C, 73.45; H, 7.48; N, 14.97.

4,4′-(2,2′-(1,3-Phenylene)bis(ethane-2,1-diyl))bis(6-methylpyridin-2-amine) (3i). Inhibitor **3i** was synthesized using general method B (85%): ^{1}H NMR (500 MHz, $CDCl_3$) δ 2.33 (s, 6H), 2.46 (br s, 4H), 2.69−2.72 (m, 4H), 2.81−2.84 (m, 4H), 6.10 (s, 2H), 6.35 (s, 2H), 6.91 (s, 2H), 6.99−7.00 (d, J = 8.0 Hz, 2H), 7.17−7.20 (m, 1H); ^{13}C NMR (125 MHz, $CDCl_3$) δ 23.8, 36.6, 37.4, 105.9, 114.1, 126.4, 128.7, 128.8, 141.5, 153.5, 156.1, 158.2; LC-TOF ($M + H^+$) calcd for $C_{22}H_{27}N_4$ 347.223 57, found 347.223 89. Anal. Calcd for $C_{22}H_{26}N_4 \cdot 0.5CH_3OH$: C, 74.55; H, 7.79; N, 15.46. Found: C, 73.49; H, 7.36; N, 14.79.

6,6′-(2,2′-(Pyridine-3,5-diyl)bis(ethane-2,1-diyl))bis(4methylpyridin-2-amine) (3j). Inhibitor **3j** was synthesized using general method B (86%): ^{1}H NMR (500 MHz, $CDCl_3$) δ 2.16 (s, 6H), 2.80−2.83 (m, 4H), 2.93−2.96 (m, 4H), 4.47 (br s, 4H), 6.17 (s, 2H), 6.27 (s, 2H), 7.31 (s, 1H), 8.26−8.27 (d, J = 1.5 Hz, 2H); ^{13}C NMR (125 MHz, $CDCl_3$) δ 21.2, 33.1, 39.6, 106.9, 114.7, 136.3, 136.8, 147.79, 147.82, 149.5, 158.6, 158.9; LC-TOF ($M + H^+$) calcd for $C_{21}H_{26}N_5$ 348.218 82, found 348.218 90. Anal. Calcd for $C_{21}H_{25}N_5 \cdot 0.5CH_3OH$: C, 71.04; H, 7.49; N, 19.27. Found: C, 70.28; H, 7.33; N, 19.11.

4-(2-(5-(2-(6-Amino-4-methylpyridin-2-yl)ethyl)pyridin-3-yl)ethyl)-6-methylpyridin-2-amine (3k). Inhibitor **3k** was synthesized using general method B (80%): ^{1}H NMR (500 MHz, $CDCl_3$) δ 2.18 (s, 3H), 2.36 (s, 3H), 2.69−2.73 (m, 2H), 2.82−2.85 (m, 4H), 2.94−2.98 (m, 2H), 4.46 (br s, 2H), 4.53 (br s, 2H), 6.09 (s, 1H), 6.19 (s, 1H), 6.31 (s, 1H), 6.35 (s, 1H), 7.27 (s, 1H), 8.26−8.29 (m, 2H); ^{13}C NMR (125 MHz, $CDCl_3$) δ 21.2, 24.2, 33.0, 33.1, 33.7, 37.0, 39.5, 105.6, 107.0, 114.1, 114.7, 136.1, 136.3, 136.8, 136.9, 147.7, 147.8, 148.1, 149.5, 149.6, 152.4, 156.8, 158.3, 158.5, 158.7, 158.8; LC-TOF ($M + H^+$) calcd for $C_{21}H_{26}N_5$ 348.218 82, found 348.218 78. Anal. Calcd for $C_{21}H_{25}N_5 \cdot 0.5CH_3OH$: C, 71.04; H, 7.49; N, 19.27. Found: C, 70.11; H, 7.30; N, 19.10.

6,6′-(2,2′-(Pyridine-2,6-diyl)bis(ethane-2,1-diyl))bis(4methylpyridin-2-amine) (3l). Inhibitor **3l** was synthesized using general method B (80%): ^{1}H NMR (500 MHz, $CDCl_3$) δ 2.14 (s, 6H), 2.97−3.01 (m, 4H), 3.13−3.16 (m, 4H), 4.68 (br s, 4H), 6.15 (s, 2H), 6.34 (s, 2H), 6.93−6.95 (d, J = 7.5 Hz, 2H), 7.41−7.44 (dd, J = 7.5, 7.5 Hz, 1H); ^{13}C NMR (125 MHz, $CDCl_3$) δ 21.2, 38.2, 38.5, 106.7, 114.5, 120.3, 136.6, 149.3, 158.6, 159.7, 161.1; LC-TOF ($M + H^+$) calcd for $C_{21}H_{26}N_5$ 348.218 82, found 348.218 71. Anal. Calcd for $C_{21}H_{25}N_5 \cdot 0.5CH_3OH$: C, 71.04; H, 7.49; N, 19.27. Found: C, 69.80; H, 7.23; N, 19.01.

4-(2-(6-(2-(6-Amino-4-methylpyridin-2-yl)ethyl)pyridin-2-yl)ethyl)-6-methylpyridin-2-amine (3m). Inhibitor **3m** was synthesized using general method B (88%): ^{1}H NMR (500 MHz, $CDCl_3$) δ 2.17 (s, 3H), 2.34 (s, 3H), 2.89−2.92 (m, 2H), 2.99−3.06 (m, 4H), 3.13−3.17 (m, 2H), 4.40 (br s, 2H), 4.43 (br s, 2H), 6.10−6.18 (m, 2H), 6.37−6.40 (m, 2H), 6.87−6.90 (dd, J = 8.0, 8.0 Hz, 1H), 6.95−6.98 (dd, J = 8.0, 8.0 Hz, 1H), 7.42−7.46 (m, 1H); ^{13}C NMR (125 MHz, CD_3OD) δ 19.9, 22.2, 35.3, 37.5, 37.6, 37.9, 105.7, 106.8, 112.9, 113.4, 120.8, 120.9, 121.0, 137.46, 137.55, 150.0, 153.3, 155.3, 158.0, 159.3, 159.5, 160.3, 160.4, 160.8; LC-TOF ($M + H^+$) calcd for $C_{21}H_{26}N_5$ 348.21882, found 348.21880. Anal. Calcd for $C_{21}H_{25}N_5 \cdot 0.5CH_3OH$: C, 71.04; H, 7.49; N, 19.27. Found: C, 70.77; H, 7.33; N, 19.21.

6,6′-(2,2′-(5-Amino-1,3-phenylene)bis(ethane-2,1diyl))bis(4-methylpyridin-2-amine) (3n). Inhibitor **3n** was synthesized

using general method B (85%): ^{1}H NMR (500 MHz, $CDCl_3$) δ 2.20 (s, 6H), 2.83−2.84 (t, J = 2.5 Hz, 8H), 3.49 (s, 2H), 4.49 (br s, 4H), 6.19 (s, 2H), 6.35 (s, 2H), 6.43 (s, 2H), 6.52 (s, 1H); ^{13}C NMR (125 MHz, $CDCl_3$) δ 21.3, 36.3, 39.9, 106.8, 113.2, 114.6, 119.5, 143.3, 146.6, 149.7, 158.2, 159.5; LC-TOF-MS ($M + H^+$) calcd for $C_{22}H_{28}N_5$ 362.234 47, found 362.233 99. Anal. Calcd for $C_{22}H_{27}N_5 \cdot 0.5CH_3OH$: C, 71.58; H, 7.74; N, 18.55. Found: C, 69.21; H, 7.33; N, 17.46.

NOS Inhibition Assays. IC_{50} values for inhibitors **3a**−**n** were measured for three different isoforms of NOS including rat nNOS, bovine eNOS, and murine macrophage iNOS using L-arginine as a substrate. The three enzyme isoforms were recombinant enzymes overexpressed (in *E. coli*) and isolated as reported.[18] These enzymes are known to have very high sequence identity. The formation of nitric oxide was measured using a hemoglobin capture assay as described previously. All NOS isozymes were assayed at room temperature in a 100 mM hepes buffer (pH 7.4) containing 10 μM L-arginine, 1.6 mM $CaCl_2$, 11.6 μg/mL calmodulin, 100 μM dithiothreitol (DTT), 100 μM NADPH, 6.5 μM H_4B, and 3.0 μM oxyhemoglobin (for iNOS assays, no additional Ca^{2+} and calmodulin). The assay was initiated by the addition of enzyme, and the initial rates of the enzymatic reactions were determined on a UV−vis spectrometer by monitoring the formation of NO-hemoglobin complex at 401 nm from 0 to 60 s after mixing. The corresponding K_i values of inhibitors were calculated from the IC_{50} values using eq 1 with known K_m values (human nNOS, 1.6 μM; rat nNOS,1.3 μM; iNOS, 8.3 μM; eNOS, 1.7 μM).

$$K_i = IC_{50}/(1 + [S]/K_m) \quad (1)$$

■ ASSOCIATED CONTENT

Supporting Information. Synthesis of **5g**, Table S1, and NMR spectra of new compounds. This material is available free of charge via the Internet at http://pubs.acs.org.

■ AUTHOR INFORMATION

Corresponding Author

*For T.L.P.: phone, 949-824-7020; fax, 949-824-3280; e-mail, poulos@
uci.edu. For R.B.S.: phone, 847-491-5653; fax, 847-491-7713; e-mail, Agman@chem.northwestern.edu.

Present Addresses

●Department of Chemistry, University of Louisiana at Lafayette, Lafayette, Louisiana 70504.

▽Department of Chemistry, Lanzhou University, Lanzhou, China.

■ ACKNOWLEDGMENT

The authors are grateful to the National Institutes of Health for financial support to R.B.S. (Grant GM49725), T.L.P (Grant GM57353), and Dr. Bettie Sue S. Masters (Grant GM52419, with whose laboratory P.M. and L.J.R. are affiliated). Dr. Bettie Sue S. Masters is the Robert A. Welch Distinguished Professor in Chemistry (AQ0012). P.M. is supported by Grants 0021620806 and 1M0520 from MSMT of the Czech Republic.

■ ABBREVIATIONS USED

NO, nitric oxide; eNOS, endothelial nitric oxide synthase; nNOS, neuronal nitric oxide synthase; iNOS, inducible nitric oxide synthase; BBB, blood−brain barrier; H_4B, tetrahydrobiopterin; *n*-BuLi, *n*-butyllithium; $NH_2OH \cdot HCl$, hydroxylamine hydrochloride; LDA, lithium diisopropylamide; TMS, tetramethylsilane; LC-TOF, liquid chromatography/time-of-flight; DMF, dimethylformamide; TFA, trifluoroacetic acid; DTT, dithiothreitol

■ REFERENCES

(1) Marletta, M. A. Nitric oxide synthase structure and mechanism. *J. Biol. Chem.* **1993**, *268*, 12231–12234.

(2) Marletta, M. A. Nitric oxide synthase: aspects concerning structure and catalysis. *Cell* **1994**, *78*, 927.

(3) Hall, A. V.; Antoniou, H.; Wang, Y.; Cheung, A. H.; Arbus, A. M.; Olson, S. L.; Lu, W. C.; Kau, C. L.; Marsden, P. A. Structural organization of the human neuronal nitric oxide synthase gene (NOS1). *J. Biol. Chem.* **1994**, *269*, 33082–33090.

(4) Wang, Y.; Newton, D. C.; Marsden, P. A. Neuronal NOS: gene structure, mRNA diversity, and functional relevance. *Crit. Rev. Neurobiol.* **1999**, *13*, 21–43.

(5) Zhang, L.; Dawson, V. L.; Dawson, T. M. Role of nitric oxide in Parkinson's disease. *Pharmacol. Ther.* **2006**, *109*, 33–41.

(6) Dorheim, M. A.; Tracey, W. R.; Pollock, J. S.; Grammas, P. Nitric oxide synthase activity is elevated in brain microvessels in Alzheimer's disease. *Biochem. Biophys. Res. Commun.* **1994**, *205*, 659–665.

(7) Norris, P. J.; Waldvogel, H. J.; Faull, R. L. M.; Love, D. R.; Emson, P. C. Decreased neuronal nitric oxide synthase messenger RNA and somatostatin messenger RNA in the striatum of Huntington's disease. *Neuroscience* **1996**, *72*, 1037–1047.

(8) Sims, N. R.; Anderson, M. F. Mitochondrial contributions to tissue damage in stroke. *Neurochem. Int.* **2002**, *40*, 511–526.

(9) Hobbs, A. J.; Higgs, A.; Moncada, S. Inhibition of nitric oxide synthase as a potential therapeutic target. *Annu. Rev. Pharmacol.* **1999**, *39*, 191–220.

(10) Southan, G. J.; Szabo, C. Selective pharmacological inhibition of distinct nitric oxide synthase isoforms. *Biochem. Pharmacol.* **1996**, *51*, 383–394.

(11) Babu, B. R.; Griffith, O. W. Design of isoform-selective inhibitors of nitric oxide synthase. *Curr. Opin. Chem. Biol.* **1998**, *2*, 491–500.

(12) Alderton, W. K.; Cooper, C. E.; Knowles, R. G. Nitric oxide synthase: structure, function and inhibition. *Biochem. J.* **2001**, *357*, 593–615.

(13) Salerno, L.; Sorrenti, V.; Di Giacomo, C.; Romeo, G.; Siracusa, M. A. Progress in the development of selective nitric oxide synthase (NOS) inhibitors. *Curr. Pharm. Des.* **2002**, *8*, 177–200.

(14) Alcaraz, M. J.; Guillén, M. I. The nitric oxide related therapeutic phenomenon: a challenging task. *Curr. Pharm. Des.* **2002**, *8*, 215–231.

(15) Vallance, P.; Leiper, J. Blocking NO synthesis: how, where and why? *Nat. Rev. Drug Discovery* **2002**, *1*, 939–950.

(16) Ji, H.; Erdal, E. P.; Litzinger, E. A.; Seo, J.; Zhu, Y.; Xue, F.; Fang, J.; Huang, J.; Silverman, R. B. *Frontiers in Medicinal Chemistry*; Reitz, A. B., Choudhary, M. I., Atta-ur-Rahman, Eds.; Bentham Science Publishers: Oak Park, IL, 2009; Vol. 5, pp 842−882.

(17) Silverman, R. B. Design of selective neuronal nitric oxide synthase inhibitors for the prevention and treatment of neurodegenerative diseases. *Acc. Chem. Res.* **2009**, *42*, 439–451.

(18) Delker, S. L.; Ji, H.; Li, H.; Jamal, J.; Fang, J.; Xue, F.; Silverman, R. B.; Poulos, T. L. Unexpected binding modes of nitric oxide synthase inhibitors effective in the prevention of cerebral palsy. *J. Am. Chem. Soc.* **2010**, *132*, 5437–5442.

(19) Lawton, G. R.; Ranaivo, H. R.; Wing, L. K.; Ji, H.; Xue, F.; Martesek, P.; Roman, L. J.; Watterson, D. M.; Silverman, R. B. Analogues of 2-aminopyridine-based selective inhibitors of neuronal nitric oxide synthase with increased bioavailability. *Bioorg. Med. Chem.* **2009**, *17*, 2371–2380.

(20) Xue, F.; Fang, J.; Lewis, W. W.; Martasek, P.; Roman, L. J.; Silverman, R. B. Potent and selective neuronal nitric oxide synthase inhibitors with improved cellular permeability. *Bioorg. Med. Chem. Lett.* **2010**, *20*, 554–557.

(21) Xue, F.; Huang, J.; H., Li; Ji, H.; Fang, J.; Poulos, T, L.; Silverman, R. B. Structure-based design, synthesis, and biological evaluation of lipophilic-tailed monocationic inhibitors of neuronal nitric oxide synthase. *Bioorg. Med. Chem.* **2010**, *18*, 6526–6537.

(22) Xue, F.; Li, H.; Fang, J.; Poulos, T. L.; Silverman, R. B. Peripheral but crucial: the hydrophobic pocket (Tyr706, Leu337, and Met336) for potent and selective inhibition of neuronal nitric oxide synthase. *Bioorg. Med. Chem. Lett.* **2010**, *20*, 6258–6261.

(23) Xue, F.; Gu, W.; Silverman, R. B. A concise route to the chiral pyrrolidine core of selective inhibitors of neuronal nitric oxide synthase. *Org. Lett.* **2009**, *11*, 5194–5197.

(24) Hagmann, W. K.; Caldwell, C. G.; Chen, P.; Durette, P. L.; Esser, C. K.; Lanza, T. J.; Kopka, I. E.; Guthikonda, R.; Shah, S. K.; MacCoss, M.; Chabin, R. M.; Fletcher, D.; Grant, S. K.; Green, B. G.; Humes, J. L.; Kelly, T. M.; Luell, S.; Meurer, R.; Moore, V.; Pacholok, S. G.; Pavia, T.; Williams, H. R.; Wong, K. K. Substituted 2-aminopyridines as inhibitors of nitric oxide synthases. *Bioorg. Med. Chem. Lett.* **2000**, *10*, 1975–1978.

(25) Momenteau, M.; Mispelter, J.; Loock, B.; Lhoste, J. M. Both-faces hindered porphyrins. Part 2. Synthesis and characterization of internally five-co-ordinated iron(II) basket-handle porphyrins derived from 5,10,15,20-tetrakis(*o*-hydroxyphenyl)porphyrin. *J. Chem. Soc., Perkin Trans. 1* **1985**, 61–70.

(26) Hevel, J. M.; Marletta, M. A. Nitric-oxide synthase assays. *Methods Enzymol.* **1994**, *233*, 250–258.

(27) Delker, S. L.; Xue, F.; Li, H.; Jamal, J.; Silverman, R. B.; Poulos, T. L. Role of zinc in isoform-selective inhibitor binding to neuronal nitric oxide synthase. *Biochemistry* **2010**, *49*, 10803–10810.

(28) Fang, J.; Silverman, R. B. A cellular model for screening neuronal nitric oxide synthase inhibitors. *Anal. Biochem.* **2009**, *390*, 74–78.

(29) Linnet, K.; Ejsing, T. B. A review on the impact of P-glycoprotein on the penetration of drugs into the brain. Focus on psychotropic drugs. *Eur. Neuropsychopharmacol.* **2008**, *18*, 157–169.

(30) Juliano, R. L; Ling, V. A. A surface glycoprotein modulating drug permeability in Chinese hamster ovary cell mutants. *Biochim. Biophys. Acta* **1976**, *455*, 152–162.

(31) Schinkel, A. H.; Mayer, U.; Wagenaar, E.; Mol, C. A.; van Deemter, L.; Smit, J. J.; van der Valk, M. A.; Voordouw, A. C.; Spits, H.; van Tellingen, O.; Zijlmans, J. M.; Fibbe, W. E.; Borst, P. Normal viability and altered pharmacokinetics in mice lacking mdr1-type (drug-transporting) P-glycoproteins. *Proc. Natl. Acad. Sci. U.S.A.* **1997**, *94*, 4028–4033.

(32) Schinkel, A. H. P-Glycoprotein, a gatekeeper in the blood-brain barrier. *Adv. Drug Delivery Rev.* **1999**, *36*, 179–194.